

Theoretical Study of Photon Emission from Molecular Wires

John Buker and George Kirczenow

Department of Physics, Simon Fraser University, Burnaby, British Columbia, Canada, V5A 1S6

(October 30, 2018)

Abstract

We explore theoretically the principles that govern photon emission from single-molecule conductors carrying electric currents between metallic contacts. The molecule and contacts are represented by a generic tight-binding model. The electric current is calculated using Landauer theory and the photon emission rate is obtained using Fermi's golden rule. The bias-dependence of the electronic structure of the molecular wire is included in the theory in a simple way. Conditions under which significant photon emission should occur are identified and photon spectra are calculated. We predict the photon emission rate to be more sensitive than the electric current to coupling asymmetries between the molecule and contacts. This has important implications for the design and interpretation of STM experiments searching for electroluminescence from individual molecules. We discuss how electroluminescence may be used to measure important characteristics of the electronic structure of molecular wires such as the HOMO-LUMO gap and location of the Fermi level of the contacts relative to the HOMO and LUMO. The feasibility of observing photon emission from Au/benzene-dithiolate molecular wires is also discussed.

PACS: 78.67.Lt, 78.60.Fi, 73.63.Rt

arXiv:cond-mat/0211357v1 18 Nov 2002

I. INTRODUCTION

A molecular wire is a single molecule (or a few molecules) that forms an electrically conducting bridge between a pair of metallic nano-contacts. In recent years molecular wires have been realized in the laboratory and their electronic transport properties have been measured¹⁻⁷. There have also been many theoretical advances in modeling such systems^{2,8-31} and the study of transport in molecular wires continues to be an active area of experimental and theoretical research³². It has been found that the current flowing through a molecular wire depends strongly on the electronic structure of the molecule as well as the geometry of the molecule and contacts and the chemical bonding between them^{8-15,19,22-25,27-31}. In a simplified picture, when a potential bias is applied to the contacts, the electrochemical potentials of the contacts separate and molecular orbitals located in the window of energy between the two electrochemical potentials mediate electron flow from one contact to the other. The current rises sharply each time this window of energy expands to include an additional molecular orbital.

Much work has been done modeling and attempting to understand I-V characteristics that have been obtained experimentally^{2,14,17,19,21,24,26,30}. No theoretical studies have been reported, however, of another potentially important property of self-assembled molecular wires, namely, photon emission (electroluminescence) from a molecular wire carrying an electric current due to electronic transitions between molecular orbitals. When a bias voltage is applied to the contacts, the molecular wire moves out of equilibrium, with a flux of electrons passing through it. Electrons enter the molecule from the contact with the higher electrochemical potential, and drain into the other contact. Since the electrochemical potentials of the contacts are no longer the same, one can no longer assume that the orbitals of the molecule will be filled up to an energy equal to a common Fermi energy of the contacts. The passage of electrons through the molecule may lead to partial occupation of various different molecular orbitals that lie within the electrochemical potential window of the contacts. It is possible that transitions from one partially occupied molecular orbital to another of lower energy occur, resulting in photon emission.

Although definitive experimental evidence of this effect has not yet been reported, related phenomena have been observed in scanning tunneling microscopy (STM) experiments: Systems with an STM tip over a clean metallic surface are known to emit photons due to the decay of plasmons³³. Recent STM experiments on molecular monolayers adsorbed on metal substrates have suggested that a different, molecule-dependent photon emission process may also occur: Poirier has reported molecule-dependent photon emission in an STM experiment involving reduced and oxidized alkanethiol monolayers adsorbed on Au(111)³⁴. In an STM experiment involving monolayer films of C₆₀ fullerenes on Au(110) surfaces, Berndt *et al.* observed enhanced photon emission when the STM tip was placed above an individual molecule³⁵. Smolyaninov has reported photon emission at energies similar to copper phthalocyanine (CuPc) transition energies in STM experiments involving CuPc adsorbed on Au³⁶. However, in very recent STM experiments by Hoffmann *et al.* on hexa-tert-butyl-decacyclene on noble-metal surfaces³⁷, it was found that while the presence of the molecules modulated the photon emission, the observed emission appeared to be plasmon-mediated rather than molecular in character. Thus, the nature of photon emission mechanisms for STM-molecular monolayer systems is yet to be adequately understood.

In all of these STM experiments, a bias voltage was applied between the STM tip and metallic surface, with a molecular monolayer interposed between these two contacts as in molecular wire systems. However, there are important differences between these STM molecular monolayer systems and self-assembled molecular wires: The coupling between the STM tip and the molecule is usually very small compared to the coupling between the molecule and the substrate, whereas for self-assembled molecular wires that are bonded chemically to both metal contacts, the couplings of the molecule to the source and drain may be comparable in strength. Also, the STM experiments involve planar metallic substrates, which are quite different from the nanoscopic metallic contacts of some self-assembled molecular wires. It is unclear how these differences would affect photon emission, so it is of interest to consider photon emission not only from STM-molecular monolayer systems but also from more symmetrically coupled self-assembled molecular wires.

Electroluminescence from molecular wires is a potentially important effect, not only because of its intrinsic fundamental interest, but also as a novel experimental probe of molecular nano-electronic devices. For example, as we will show below, by observing the photon emission spectrum of a molecular wire, important information about its the electronic structure, including the energies of the molecular orbitals, their locations relative to the Fermi level, and their occupations as a function of bias voltage, may in principle be obtained. There is currently disagreement between different theoretical models of 1,4 benzene-dithiolate (BDT) attached to gold contacts^{14,19,21,25,28,30} regarding the energies of the highest occupied molecular orbital (HOMO) and the lowest unoccupied molecular orbital (LUMO), relative to the Fermi level of the contacts. If the photon emission spectra of such systems were modelled, and compared with experiment, important new insights into the most appropriate models for molecular wires could be obtained.

In this article, we present and solve a generic model for photon emission from a molecular wire. As this is the first theoretical study of this effect, our purpose will be to develop a basic qualitative picture of the underlying mechanism, and to examine how adjustment of the various model parameters, to reflect different experimental situations, should affect photon emission. We use a one-dimensional tight-binding model that attempts to capture the important physics involved in a way that is simple and intuitively reasonable, and is qualitatively consistent with what is already known about molecular wire electronic structure and transport. Another objective of this work is to provide some guidance to experimentalists as to which types of systems to study in order to observe photon emission. We find that, under certain circumstances, the model predicts that photon emission should occur, due to molecular orbital transitions. We show how molecular orbital occupations behave as a function of applied bias voltage, and how varying the model parameters changes this behaviour. Fermi's Golden Rule is used to calculate photon emission spectra. We show how the emission depends on molecular orbital occupations, and the locations of the molecular orbitals relative to the Fermi levels of the contacts.

Our model and theoretical approach are described in Section II. The results of our calculations and their interpretation are presented in Section III. We conclude in Section IV by summarizing our results, and discussing their implications for possible experiments directed at observing photon emission from BDT attached to gold contacts.

II. THE MODEL

Each metal contact will be modelled as a one-dimensional tight-binding chain. The molecular wire is modelled as a pair of atoms placed next to the origin, forming a bridge between the two contacts (see Fig. 1). The model Hamiltonian of this system is

$$\begin{aligned}
H = & \sum_{n<0} \epsilon_L |n\rangle\langle n| + \beta(|n-1\rangle\langle n| + |n\rangle\langle n-1|) \\
& + \sum_{n>0} \epsilon_R |n\rangle\langle n| + \beta(|n+1\rangle\langle n| + |n\rangle\langle n+1|) \\
& + \epsilon_a |a\rangle\langle a| + \epsilon_b |b\rangle\langle b| + \beta_{-1,a}(|-1\rangle\langle a| + |a\rangle\langle -1|) \\
& + \beta_{1,b}(|1\rangle\langle b| + |b\rangle\langle 1|) + \beta_{a,b}(|a\rangle\langle b| + |b\rangle\langle a|)
\end{aligned} \tag{1}$$

where ϵ_L and ϵ_R are the site energies of the left (source) and right (drain) contacts, and ϵ_a and ϵ_b are the site energies of atoms a and b of the molecule, which depend on the bias voltage applied to the wire and the nature of the metal contacts, as well as the identities of atoms a and b . β , $\beta_{-1,a}$, $\beta_{1,b}$ and $\beta_{a,b}$ are the hopping amplitudes between atoms in the contacts, between atom a of the molecule and the left contact, between atom b and the right contact, and between atom a and atom b , respectively. $|n\rangle$ represents the orbital of an atom in one of the contacts, and $|a\rangle$ and $|b\rangle$ represent the atomic orbitals of the molecule. We consider the orbitals of different atoms to be orthogonal. However, this model may easily be extended to systems where this is not the case¹⁶. We take the the electrochemical potentials of the source and drain contacts to be $\mu_S = E_F + eV_{bias}/2$ and $\mu_D = E_F - eV_{bias}/2$ where V_{bias} is the bias voltage applied between them and E_F is their common Fermi level at zero applied bias. The applied bias also affects the site energies ϵ_L and ϵ_R of the contacts so that $\epsilon_L = \epsilon_{contacts} + eV_{bias}/2$ and $\epsilon_R = \epsilon_{contacts} - eV_{bias}/2$, where $\epsilon_{contacts}$ is the zero bias site energy. Our treatment of the effect of the bias voltage on site energies ϵ_a and ϵ_b of the molecule itself is described at the end of Section II.

Electrons exist in the form of Bloch waves in the contacts, and undergo reflection or transmission when they encounter the two-atom molecule. Their wavefunctions are of the form

$$|\psi\rangle = \sum_{n<0} (e^{iknd} + re^{-iknd})|n\rangle + \sum_{n>0} te^{ik'nd}|n\rangle + c_a|a\rangle + c_b|b\rangle \tag{2}$$

where d is the lattice spacing, and t and r are the transmission and reflection coefficients. The electrons have eigenenergies of the form $E = \epsilon_i + 2\beta\cos(kd)$. This equation holds for both $\epsilon_i = \epsilon_L$ and $\epsilon_i = \epsilon_R$, so when an electron with initial wavevector k undergoes transmission, its wavevector changes (to k') due to the difference between ϵ_L and ϵ_R . For certain k , there are no real solutions for k' . In these cases, k' becomes complex, and the transmitted Bloch wave is evanescent. By applying $\langle -1|$, $\langle a|$, $\langle b|$, and $\langle 1|$ to $H|\psi\rangle$, analytic expressions for the transmission and reflection coefficients are obtained:

$$t = \frac{2i\beta_{-1,a}\beta_{1,b}\beta_{a,b}\beta\sin(kd)}{\beta_{a,b}^2\beta^2 - [\beta(E - \epsilon_b) - \beta_{1,b}^2e^{ik'd}][\beta(E - \epsilon_a) - \beta_{-1,a}^2e^{ikd}]} \tag{3}$$

$$r = -\frac{[\beta(E - \epsilon_a) - \beta_{-1,a}^2e^{-ikd}][\beta(E - \epsilon_b) - \beta_{1,b}^2e^{ik'd}] - \beta_{a,b}^2\beta^2}{[\beta(E - \epsilon_a) - \beta_{-1,a}^2e^{ikd}][\beta(E - \epsilon_b) - \beta_{1,b}^2e^{ik'd}] - \beta_{a,b}^2\beta^2} \tag{4}$$

The coefficients c_a and c_b for the atomic orbitals in the molecule are similarly obtained, in terms of the transmission and reflection coefficients:

$$c_a = \frac{\beta(1+r)}{\beta_{-1,a}}, \quad c_b = \frac{\beta t}{\beta_{1,b}} \quad (5)$$

The transmission probability is given by

$$T = |t|^2 \frac{v(k')}{v(k)} = |t|^2 \frac{\sin(k'd)}{\sin(kd)} \quad (6)$$

where $v(k)$ is the velocity of the incoming wave and $v(k')$ is the velocity of the transmitted wave. In our model, T depends on the energy of the incoming electron, as well as on V_{bias} . The V_{bias} dependence arises from the effect of V_{bias} on the site energies of the contacts (described above) and of the molecule that will be discussed below. Using Landauer theory³⁸, an expression for the current is obtained:

$$I = \frac{2e}{h} \int_{\mu_D}^{\mu_S} T(E, V_{bias}) dE \quad (7)$$

Here we assume the temperature to be 0 K, so the Fermi functions are trivial, and the transmission probability is only integrated through the Fermi energy window.

To calculate emission spectra for the molecular wire we use the expression for the spontaneous emission rate of a system emitting photons into empty space, using Fermi's Golden Rule³⁹. The emission rate is given by

$$\frac{4e^2\omega^3}{3\hbar c^3} |\langle \psi_f | \mathbf{x} | \psi_i \rangle|^2 \quad (8)$$

where ψ_i and ψ_f represent initial and final states, and $\hbar\omega$ is their difference in energy. We consider emission only from the molecular sites a and b . The emission rate is therefore approximated by

$$R = \frac{4e^2\omega^3}{3\hbar c^3} |c_{a,f}^* c_{a,i} \langle a | \mathbf{x} | a \rangle + c_{b,f}^* c_{b,i} \langle b | \mathbf{x} | b \rangle|^2 \quad (9)$$

where i and f label initial and final states. The overlap terms $\langle a | \mathbf{x} | b \rangle$ and $\langle b | \mathbf{x} | a \rangle$ are neglected since they should be small compared to $\langle a | \mathbf{x} | a \rangle$ and $\langle b | \mathbf{x} | b \rangle$. We approximate $\langle a | \mathbf{x} | a \rangle$ and $\langle b | \mathbf{x} | b \rangle$ by the locations of their atomic centers, so that $\langle a | \mathbf{x} | a \rangle = -\frac{b}{2}$, $\langle b | \mathbf{x} | b \rangle = \frac{b}{2}$ (b being the molecular bond length). Thus, we have

$$R(k_i, \omega) = \frac{e^2\omega^3 b^2}{3\hbar c^3} |c_{b,f}^* c_{b,i} - c_{a,f}^* c_{a,i}|^2 \quad (10)$$

To calculate the emission rate as a function of photon energy, we must consider all electron states of the system, incoming from both the source and drain contacts. Since we assume the temperature to be 0 K, all states up to the electrochemical potential of the appropriate contact are occupied. ψ_f must be initially unoccupied, and it must be of lower energy than ψ_i . Therefore, we consider transitions from occupied initial states that are incoming from the source, to final states, within the electrochemical potential window, that are incoming from the drain. After normalizing the wavefunctions and converting the sum over k -states

(and spin) into an integral over energy, an expression for the photon emission spectrum (for a given bias voltage) is obtained:

$$f(\omega) = \frac{1}{2\pi} \int_{\mu_D + \hbar\omega}^{\mu_S} \frac{R(k_i, \omega)}{-\beta \sin(k_i d)} dE_i \quad (11)$$

In order to interpret our results physically, it is useful to relate the emission spectra to total occupations of the molecular orbitals, as a function of bias voltage. For this purpose, we project eigenstates of the system given by equation (2) onto the bonding and antibonding orbitals of the isolated molecule, whose coefficients will be labelled c_O and c_{O^*} respectively. Their total occupations are calculated by summing over all occupied electron states (including spin) incoming from both contacts. This sum is converted into an integral, and an expression for the total bonding and antibonding orbital occupations (O, O^*) is obtained:

$$(O, O^*) = \frac{1}{2\pi} \sum_{\text{contacts } i} \int \frac{|c_O, c_{O^*}|^2}{-\beta \sin(k_i d)} dE_i \quad (12)$$

Changes in the occupations of the bonding and antibonding orbitals in response to changes of the applied bias voltage may result in some charging of the molecule. If this occurs, the charging causes an electrostatic shift of the molecular energy levels that in turn severely limits the actual charging that takes place²³. In the present work we approximate the shift of the molecular levels in response to the applied bias by adjusting ϵ_a and ϵ_b equally so as to maintain the net charge that the molecule has at zero bias. The simplicity of this approximation is in keeping with the generic nature of the molecular wire model that we consider here. It yields behavior of the molecular levels with bias that is physically reasonable, and as will be seen in Section III B, remarkably similar to that obtained from *ab initio* calculations for some molecular wire systems.

In the remainder of this article we will consider the case where the Fermi level of the leads at zero bias falls within the HOMO-LUMO gap of the molecule, as is typical of molecular wires such as the Au/benzene-dithiolate/Au system. Thus we will identify the bonding and antibonding orbitals O and O^* with the HOMO and LUMO, respectively, of the isolated molecule. (The terms O and HOMO will henceforth be used interchangeably as will O^* and LUMO.) Our model parameters will be chosen so that at zero bias the Fermi level of the leads lies between O and O^* . As will be seen below, if the Fermi level is well above O and well below O^* (but O and O^* are within the electronic energy band of the leads) it follows from Eq. 12 that at zero bias O is almost completely filled with electrons and O^* is almost empty, although O is never *totally* full and O^* is never completely empty because of the level broadening that occurs due to hybridization between the states of the molecule and leads. In this way the HOMO and LUMO character of the O and O^* orbitals is expressed within our model when the molecule couples to the leads. By choosing different values of the site energies ϵ_a and ϵ_b at zero bias, the energies and occupations of the O and O^* orbitals can be varied. Thus the effects of differing amounts of charge transfer between the molecule and leads can also be studied within our model.

We also note in passing that although our results are described here in terms of electron transport and optical transitions between occupied and empty electron states, an equivalent description can be given in terms of electron and hole transport and optical transitions.

III. RESULTS

We consider the case where the energy bands of the contacts are partially filled ($k_F = \frac{\pi}{2d}$). In numerical results presented below the hopping parameters are chosen to have values typical of molecular wire systems ($\beta = -5$ eV, $\beta_{a,b} = -1.5$ eV), resulting in a HOMO LUMO gap of 3 eV for the isolated molecule.

A. Symmetric molecule-contact couplings; HOMO LUMO gap centred at E_F .

In this section, The HOMO-LUMO gap of the molecule is chosen to be centred at the zero bias Fermi level of the contacts, and the molecule-contact couplings have equal values. First, we consider the case where these couplings have values similar to those in chemically bonded molecular wire systems ($\beta_{-1,a} = \beta_{1,b} = -1.0$ eV). Fig. 2a shows how the source and drain electrochemical potentials μ_S and μ_D and the energies of the bonding (O) and antibonding (O^*) orbitals behave as a bias is applied to the contacts. At zero bias, O is located at -1.5 eV and O^* at +1.5 eV. Fig. 2b shows the electron transmission probability through the molecule at zero bias obtained from eq. 6. The bonding and antibonding orbitals provide channels for electron transmission, so there are peaks at electron energies of -1.5 eV and +1.5 eV. The transmission peaks are somewhat broadened due to the coupling of the molecule to the contacts, which causes the discrete molecular orbitals (O and O^*) to hybridize with the continuum of states in the contacts. Returning to Fig. 2a, as V_{bias} increases, the electrochemical potentials of the source (μ_S) and drain (μ_D) separate. At $V_{bias} = 3$ V, μ_S moves above O^* and μ_D moves below O . In this symmetric case, this does not result in any change in the energies of O and O^* . Fig. 2c shows the electron occupation of the molecular wire, as projected onto the bonding (O) and antibonding (O^*) orbitals of the isolated molecule. At zero bias, O is almost fully occupied, and O^* is almost empty. As V_{bias} increases, O partially empties. μ_D moves below O in energy, so electrons from the drain no longer contribute to the filling of the bonding orbital, while electrons from the source continue to contribute, so O becomes half-filled. Similarly, electrons from the source start to fill O^* as μ_S approaches O^* in energy, and finally O^* becomes half-filled as well. As O and O^* empty and fill with V_{bias} , the total occupation remains constant (two electrons), due to the symmetric placement of E_F , at the centre of the HOMO LUMO gap. Therefore, there is no tendency for the molecule to charge, and the orbital energies remain constant (Fig. 2a). Notice that the filling and emptying of O and O^* , as a function of V_{bias} , is gradual. This is due to the fact that the continuous density of states associated with the broadened resonances in Fig. 2b enters the electrochemical potential window between μ_S and μ_D gradually. Fig. 2d shows the orbital occupation for the case of weak molecule-contact coupling ($\beta_{-1,a} = \beta_{1,b} = -0.2$ eV). The weak coupling results in a more sharply peaked molecular density of states, so O and O^* empty and fill much more abruptly. Fig. 2e shows the resulting total photon emission rate for (i) $\beta_{-1,a} = \beta_{1,b} = -0.2$ eV and (ii) $\beta_{-1,a} = \beta_{1,b} = -1.0$ eV. Emission is strong when the energies of O and O^* are inside the electrochemical potential window. In case (i), emission increases more rapidly with bias near $V_{bias} = 3.0$ V than in case (ii), because O and O^* empty and fill more abruptly. Fig. 2f shows how, within our model, the emission spectrum for case (ii) changes with bias. As expected, emission is peaked around the transition energy of the molecule (3 eV) at higher

bias. (Weaker molecule-contact couplings would result in more sharply peaked emission spectra, due to weaker hybridization and broadening of molecular orbitals.) Since photons cannot be emitted at energies higher than eV_{bias} the spectra cut off at this energy. This is one of the factors that contributes to the noticeable shift of the emission peak upwards in energy with increasing V_{bias} . Another factor contributing to this blue shift is the cubic dependence of the emission rate on the photon energy $\hbar\omega$ in equation (9). This explains the significant photon emission seen in Fig. 2f for $V_{bias} = 6$ V at energies well above the molecule's nominal HOMO-LUMO gap energy, due to transitions from the higher energy tail of O^* , and to the lower energy tail of O .

B. Symmetric molecule-contact couplings; E_F close to HOMO or LUMO.

In many experimental situations, the HOMO-LUMO gap is not centred at the Fermi level of the contacts. Often, either the HOMO or LUMO is close to E_F ^{21,25,28}. In Fig. 3a, O has a zero bias energy located just below E_F . In our model, as V_{bias} increases, O and O^* first decrease in energy following μ_D . Then, at around 3 V, as the energy of O^* approaches μ_S , O and O^* begin to rise in energy with μ_S . The opposite situation occurs when O^* has a zero bias value just above E_F (Fig. 3b). In this case, O and O^* first rise in energy with μ_S , then fall with μ_D after $V_{bias} = 3$ V. This behaviour is nearly identical to recent results obtained through self-consistent density-functional calculations for the HOMO and LUMO energies of a gold nanowire attached to two gold contacts²⁹, suggesting that our model's approach to charging can be quite a good approximation for some molecular wires. Fig. 3c shows the orbital occupations for the case of O just below E_F in energy at zero bias (same situation as Fig. 3a). The total occupation is less than 2 electrons (1.6 electrons) due to the fact that, at zero bias, O is very close to E_F , so that its high energy tail is above E_F and is unoccupied. As μ_D decreases, the molecular orbitals drop in energy so that the total molecular charge is maintained at its zero bias value. Eventually, as μ_S increases, it approaches the antibonding energy, causing O^* to start to fill. The orbitals stop dropping in energy, so that any filling of O^* is accompanied by an emptying of O . Once O is significantly above μ_D , its occupation becomes constant with further changes in bias, at about 1 electron, as only the source contact contributes electrons. Both orbitals now move upwards in energy, causing O^* to stop filling so that the total charge is still maintained at its zero bias value. The high energy tail of O^* stays above μ_S , so that the orbital only fills to about 0.6 electrons. Fig. 3d similarly shows the orbital occupations for the case of O^* just above E_F at zero bias (the situation in Fig. 3b). In this case, the total occupation is more than 2 electrons (2.4 electrons) due to the fact that O^* is partially occupied at zero bias, because its low energy tail is below E_F . O partially empties and O^* partially fills as the orbitals enter the electrochemical potential window at a bias voltage near 3 V. The occupation of O^* becomes about 1 electron, coming from the source contact. The occupation of O is greater (1.4 electrons) because the low energy tail of O is still below μ_D . Fig. 3e shows the total emission rate predicted by our model for the case where O is just below E_F at zero bias. A nearly identical emission rate is predicted for the case of O^* just above E_F . In both cases, emission becomes strong above $V_{bias} = 3$ V. This is the point at which O and O^* enter the electrochemical potential window, and therefore are both partially occupied. Emission at high bias is less than half as strong as in the case of HOMO and LUMO that are symmetric about E_F (Fig. 2), due to the fact

that either O^* is not as highly occupied (Fig. 3c) or O is not as empty (Fig. 3d), as in Fig. 2c. Fig. 3f shows the emission spectrum for the case of O just below E_F at zero bias, for $V_{bias} = 6$ V. (A very similar spectrum is predicted for the case of O^* just above E_F .) The spectrum is not blue-shifted as strongly as in Fig. 2f, because the higher energy tail of O^* remains unoccupied (Fig. 3a) (or the lower energy tail of O remains fully occupied (Fig. 3b)), resulting in fewer high energy transitions.

C. Asymmetric molecule-contact couplings; HOMO-LUMO gap centred at E_F .

By examining the effects of varying $\beta_{-1,a}$ and $\beta_{1,b}$ we are also able to explore the behavior of photon emission from molecular wires with asymmetric molecule-contact couplings, such as systems where one of the contacts is an STM tip. In this section, we consider the case where the HOMO-LUMO gap of the molecule is centred at the zero bias Fermi level of the contacts. First, we consider highly asymmetric couplings: $\beta_{-1,a} = -0.1$ eV, $\beta_{1,b} = -1.0$ eV. Fig. 4 shows how O and O^* change in energy as a function of bias. The coupling of the molecule to the drain is much greater than to the source, so the drain has a much greater effect on orbital occupations. As V_{bias} increases from 0 V, the energy levels of O and O^* drop at the same rate as μ_D . In this way the occupations of O (although a part of its high energy tail is above μ_D) and O^* (due to the part of its low energy tail that is below μ_D) change little, and the total charge is maintained at its zero bias value. As O^* crosses μ_S in energy, its occupation increases very slightly. This causes a slight deviation of the orbital energies from a straight line, as O empties slightly by moving closer in energy to μ_D . The occupation of O remains close to 2 electrons throughout, and O^* remains almost completely unoccupied. In agreement with this, our model predicts that photon emission is extremely weak in this situation. If the values of $\beta_{-1,a}$ and $\beta_{1,b}$ are switched, O and O^* rise in energy with μ_S instead. The orbital occupations are similar to those in the opposite situation, since this time the source has a much greater effect on occupations. So, photon emission in this reverse situation is also negligible. This lack of significant photon emission from the molecule, caused by the asymmetry of the contact couplings, is a possible explanation for the lack of molecular-based photon emission observed in recent STM-HBDC monolayer experiments by Hoffmann *et al.*³⁷.

To understand better the dependence of the photon emission on the asymmetry of the couplings, it is useful to consider an intermediate case of asymmetric couplings shown in Fig. 5: $\beta_{-1,a} = -0.6$ eV, $\beta_{1,b} = -1.0$ eV. Fig. 5a shows how the model predicts O and O^* to change in energy as a function of bias. Up to $V_{bias} = 3$ V, O and O^* change little in energy. Above $V_{bias} = 3$ V, both O and O^* descend in energy with μ_D . Fig. 5b shows the orbital occupations. For $V_{bias} < 3$ V, O^* fills significantly as it approaches μ_S . For this reason, at $V_{bias} < 3$ V, O and O^* do not drop much in energy, as they do in Fig. 4 due to the emptying of the high energy tail of O . At $V_{bias} = 3$ V, O^* partially fills as it crosses μ_S , but the drain couples more strongly to the molecule. Therefore, O and O^* are pulled down with μ_D , such that O only empties to the extent that O^* fills, so that the total charge is maintained at its zero bias level. The result is that O empties to about 1.5 electrons, and O^* fills to 0.5 electrons. Fig. 5c shows photon emission for this case, and other intermediate cases. For this case ($\beta_{-1,a} = -0.6$ eV), emission is quite drastically reduced compared to the case of symmetric couplings, but is not negligible. For the reverse situation ($\beta_{-1,a} = -1.0$

eV, $\beta_{1,b} = -0.6$ eV), the reverse arguments apply, and the result is that the emission is similar. The degree of contact coupling asymmetry clearly plays a key role in determining the strength of photon emission. Our results indicate that in order for an STM experiment to detect molecular-based photon emission, the STM tip must not be very weakly coupled with the molecule. Since coupling strength varies exponentially with coupling distance, any molecular-based photon emission observed in an STM experiment will be very sensitive to the tip-sample distance. If the tip is too far from the sample, emission will be negligible.

In order to facilitate comparison of this prediction with the results of potential experiments, it is useful to relate contact coupling asymmetry to the amount of current flowing through a molecular wire as well, because, unlike coupling strength, current is a directly measurable quantity. Fig. 5d shows how the current (obtained from eq. (7)) changes with V_{bias} for various values of $\beta_{-1,a}$, holding $\beta_{1,b}$ fixed at -1.0 eV. As O and O^* enter the Fermi energy window, these orbitals act as channels for electron transmission, and the current increases as a result. Asymmetric contact couplings result in reduced current flow. Notice, however, that the current flow is not affected by strongly asymmetric couplings as much as is the photon emission rate. Fig. 5e compares how photon emission and current depend on contact coupling asymmetry, for $V_{bias} = 6$ V. Emission has a power law dependence (roughly $\beta_{-1,a}^{3.8}$), while the dependence of the current on the asymmetry is clearly much less strong. Fig. 5f shows the calculated photon emission vs. the current, for $V_{bias} = 6$ V. At weak currents, the photon emission rapidly becomes negligible. This is an important consideration to keep in mind when attempting to observe molecular photon emission experimentally.

D. Asymmetric molecule-contact couplings; E_F close to HOMO or LUMO.

Our results suggest that, for a HOMO-LUMO gap that is symmetric about E_F , asymmetric molecule-contact couplings, such as those where one of the contacts is an STM tip, result in very low photon emission rates. We consider now strongly asymmetric couplings ($\beta_{-1,a} = -0.1$ eV, $\beta_{1,b} = -1.0$ eV) for the case of HOMO or LUMO very close to E_F at zero bias. This coupling configuration is analogous to an STM experiment performed under forward bias (the STM tip acts as the (weakly coupled) source, from which electrons flow). The opposite configuration ($\beta_{-1,a} = -1.0$ eV, $\beta_{1,b} = -0.1$ eV) is analogous to an STM experiment performed under reverse bias (the STM tip acts as the (weakly coupled) drain). Fig. 6a shows how, for the forward bias situation, O and O^* change in energy as a function of bias, for the case of O very close to E_F at $V_{bias} = 0$. O and O^* drop in energy following the electrochemical potential μ_D of the strongly coupled contact. Even as O^* crosses μ_S , the orbital energies continue to decrease almost linearly because, unlike in Fig. 4, O is very close to μ_D , so that the density of states at μ_D is high and the weak filling of O^* that occurs as it crosses μ_S can be compensated by a weak emptying of O with only a very small deviation of O from its linear behavior. Fig. 6b shows the energies of O and O^* for the case of reversed contact coupling strengths ($\beta_{-1,a} = -1.0$ eV, $\beta_{1,b} = -0.1$ eV), which is equivalent to performing an STM experiment under reverse bias. This time, O and O^* rise in energy following the electrochemical potential μ_S . O^* never approaches μ_S , so it remains empty. Fig. 6c,d show photon emission for the forward bias situation (Fig. 6a). Biases above 3 V result in a small amount of photon emission because, unlike in the case of Fig. 4, O is only partially occupied, so some transitions from O^* may occur. Emission is still weak (1-2 orders

of magnitude less than for symmetric contacts), because O^* becomes only weakly occupied when crossing the Fermi level of the weakly coupled contact μ_S . The emission spectrum, shown in Fig. 6d, is peaked at an energy slightly less than 3 eV, because the lower energy tail of O is completely filled, and may not receive transitions. In the reversed coupling situation (Fig. 6b), photon emission is negligible, since O^* never approaches μ_S and remains empty. Now we consider the cases where O^* is very close to E_F at $V_{bias} = 0$ (Fig. 6e,f). Again, the energies of O and O^* follow the Fermi level of the strongly coupled contact. Therefore, for the case of weak source contact coupling (Fig. 6e), there is negligible emission because O never crosses μ_D and remains completely filled. For the case of weak drain contact coupling (Fig. 6f), there is (weak) photon emission, because O enters the electrochemical potential window and (slightly) empties. (The emission curves for this case are very similar to Fig. 6c,d.) This property of asymmetrically coupled systems may be used to help distinguish a system where the HOMO is close to E_F from a system where the LUMO is close to E_F , with the use of an STM as the weakly coupled contact. Within our model, if the HOMO is close to E_F , the result is photon emission under high forward bias and negligible emission under reverse bias, whereas if the LUMO is close to E_F , the result is emission under high reverse bias and negligible emission under forward bias. The implications of this may be important for molecular electronics research. For example, there is currently disagreement over whether E_F is located close to the HOMO or the LUMO in the system of BDT attached to gold contacts^{14,19,21,25,28,30}. The photon emission characteristics of such a system could help determine the locations of the HOMO and LUMO, and therefore which type of model is more appropriate for such a system.

IV. CONCLUSIONS

We have examined theoretically the possibility of photon emission occurring due to molecular transitions in current-carrying molecular wires. Our results suggest that significant photon emission may occur for bias voltages near or above the HOMO-LUMO energy gap of the molecule, depending on the specifics of the electronic structure of the molecule and contacts and of the couplings between the molecule and the source and drain. The predicted photon spectra are peaked near the gap energy⁴⁰. If two molecular orbitals are located in the energy window between the electrochemical potentials of the contacts, they will both be partially occupied and, as long as transitions between the orbitals are not forbidden, transitions from the higher energy orbital to the lower energy orbital should occur, resulting in photon emission. We find that varying the strength of the molecule-contact couplings changes the emission strength and spectrum. Weak, symmetric couplings result in a sharply peaked emission spectrum. Asymmetric couplings result in reduced photon emission. Emission from strongly asymmetrically coupled systems (such as some STM-molecular monolayer systems) is predicted to be extremely weak if the zero bias value Fermi level E_F of the contacts is not close to the HOMO or LUMO energy of the molecule. If E_F is close to the HOMO or LUMO energy, the amount of photon emission observed under forward bias and under reverse bias, in an STM experiment, may be compared in order to determine which of the orbitals is close in energy to E_F .

Whether E_F is close to the HOMO or LUMO energy is a difficult unresolved issue in current research on molecular wires such as BDT attached to gold contacts; *ab initio* cal-

culations based on different models and approximations^{21,25,28} have yielded opposite results in this regard. It is believed that the HOMO and LUMO of BDT attached to gold contacts are composed of bonding and antibonding orbitals (π and π^*). The present work suggests that, if the contact couplings are symmetric, photon emission will not be drastically different whether E_F is close to the HOMO or to the LUMO: Each orbital will become partially occupied as the bias voltage becomes greater than the HOMO-LUMO gap, and, so long as $\pi^* \rightarrow \pi$ transitions are allowed, this will result in photon emission. Optical transitions are forbidden if $\langle \psi_f | \mathbf{x} | \psi_i \rangle = 0$. We have used extended Hückel theory to examine the HOMO and LUMO of BDT⁴². The contacts were not included in this calculation. By symmetry analysis of the HOMO and LUMO, we found that $\langle HOMO | y | LUMO \rangle \neq 0$, where y is in the direction of the plane of the molecule, perpendicular to the contacts. Therefore, optical transitions should be allowed, and would result in the emission of y-polarized photons. Experimental evidence of BDT optical transitions is available in the form of absorption spectra for BDT in hexane⁴³. Absorption occurs for energies higher than about 4 eV, indicating a possible experimental value for BDT's HOMO-LUMO energy gap. Transport measurements on Au/BDT/Au molecular wires have been reported at bias voltages as high as approximately 5V¹. Thus it appears to be quite reasonable to undertake an experimental search for electroluminescence due to molecular transitions in Au/BDT/Au systems. An experimental determination of the HOMO-LUMO gap of BDT in the presence of the Au contacts by this means would be an important test of the validity of various theories of molecular wires. If one of the Au contacts is an STM tip, electroluminescence measurements may also be expected to be helpful in determining the location of the Fermi level of Au relative to the HOMO and LUMO states of the molecular wire.

The study of electroluminescence from molecular wires has only just begun. We hope that the theoretical ideas presented here will stimulate further experimental and theoretical work on this interesting and potentially important topic.

This work was supported by NSERC and by the Canadian Institute for Advanced Research.

REFERENCES

- ¹ M. A. Reed, C. Zhou, C. J. Muller, T. P. Burgin, and J. M. Tour, *Science* **278**, 252 (1997).
- ² S. Datta, W. Tian, S. Hong, R. Reifenberger, J. I. Henderson, C. P. Kubiak, *Phys. Rev. Lett.* **79**, 2530 (1997).
- ³ R. M. Metzger, B. Chen and M. P. Cava, *Thin Solid Films* **327/329**, 326 (1998).
- ⁴ J. K. Gimzewski and C. Joachim, *Science* **283**, 1683 (1999).
- ⁵ J. Chen, M. A. Reed, A. M. Rawlett and J. M. Tour, *Science* **286**, 1550 (1999).
- ⁶ C. P. Collier, G. Mattersteig, E. W. Wong, Y. Luo, K. Beverly, J. Sampaio, F. M. Raymo, J. F. Stoddart and J. R. Heath, *Science* **289**, 1172 (2000).
- ⁷ J. Reichert, R. Ochs, D. Beckmann, H. B. Weber, M. Mayor and H. v. Löhneysen, *cond-mat/0106219* (2001).
- ⁸ M. P. Samanta, W. Tian, S. Datta, J. I. Henderson, and C. P. Kubiak, *Phys. Rev. B* **53**, R7626 (1996).
- ⁹ M. Kemp, A. Roitberg, V. Mujica, T. Wanta and M. A. Ratner, *J. Phys. Chem* **100**, 8349 (1996).
- ¹⁰ C. Joachim, and J. F. Vinuesa, *Europhys. Lett.* **33**, 635 (1996).
- ¹¹ V. Mujica, M. Kemp, A. Roitberg and M. Ratner, *J. Chem. Phys.* **104**, 7296 (1997).
- ¹² M. Magoga, and C. Joachim, *Phys. Rev. B* **56**, 4722 (1997).
- ¹³ S. N. Yaliraki, M. A. Ratner, *J. Chem. Phys.* **109**, 5036 (1998).
- ¹⁴ E. G. Emberly and G. Kirczenow, *Phys. Rev. B* **58**, 10911 (1998).
- ¹⁵ N. D. Lang and P. Avouris, *Phys. Rev. Lett.* **81**, 3515 (1998).
- ¹⁶ E. G. Emberly and G. Kirczenow, *Phys. Rev. Lett.* **81**, 5205 (1998); *J. Phys. Cond. Matt.* **11**, 6911 (1999).
- ¹⁷ S. N. Yaliraki, M. Kemp, and M. A. Ratner, *Jnl. Am. Chem. Soc.* **121**, 3428 (1999).
- ¹⁸ E. G. Emberly and G. Kirczenow, *Phys. Rev. B* **62**, 10451 (2000).
- ¹⁹ L. E. Hall, J. R. Reimers, N. S. Hush and K. Silverbrook, *J. Chem. Phys.* **112**, 1510 (2000).
- ²⁰ V. Mujica, A. E. Roitberg and M. A. Ratner, *J. Chem. Phys.* **112**, 6834 (2000).
- ²¹ M. Di Ventra, S. T. Pantelides and N. D. Lang, *Phys. Rev. Lett.* **84**, 979 (2000).
- ²² R. Gutierrez, F. Grossmann, O. Knospe, and R. Schmidt, *Phys. Rev. A* **64**, 13202 (2001).
- ²³ E. G. Emberly and G. Kirczenow, *Phys. Rev. B* **64**, 125318(2001).
- ²⁴ E. G. Emberly and G. Kirczenow, *Phys Rev. Lett.* **87**, 269701 (2001). E. G. Emberly and G. Kirczenow, *Phys. Rev. B* **64**, 235412 (2001).
- ²⁵ P. S. Damle, A. W. Ghosh and S. Datta, *Phys Rev. B* **64**, 201403 (2001).
- ²⁶ J. Taylor, H. Guo and J. Wang, *Phys. Rev. B* **63**, 121104 (2001).
- ²⁷ E. G. Emberly and G. Kirczenow, *Chem. Phys.* **281**, 311 (2002).
- ²⁸ P. Damle, T. Rakshit, M. Paulsson and S. Datta, *cond-mat/0206328* (2002).
- ²⁹ P. Damle, A. W. Ghosh and S. Datta, *cond-mat/0206551* (2002).
- ³⁰ A.M. Bratkovsky and P.E. Kornilovitch, *cond-mat/0204597* (2002)
- ³¹ P.E. Kornilovitch, A.M. Bratkovsky and R.S. Williams, *cond-mat/0206495* (2002).
- ³² See P. Hänggi, M. Ratner and S. Yaliraki, editors, *Chem. Phys.* **281**, issues 2-3, pages 111-502 (2002)
- ³³ R. Berndt, J. K. Gimzewski, and P. Johansson, *Phys. Rev. Lett.* **67**, 3796 (1991).
- ³⁴ G. E. Poirier, *Phys. Rev. Lett.* **86**,83 (2001).

- ³⁵ R. Berndt, R. Gaisch, J. Gimzewski, B. Reihl, R. Schlittler, W. Schneider, M. Tschudy, *Science* **262**, 1425 (1993).
- ³⁶ I. I. Smolyaninov, M. S. Khaikin, *Phys. Lett.* **149**, 410 (1990).
- ³⁷ G. Hoffmann, L. Libioulle and R. Berndt, *Phys. Rev. B* **65**, 212107 (2002).
- ³⁸ R. Landauer, *IBM J. Res. Dev.* **1**, 223 (1957); R. Landauer, *Phys. Lett.* **85A**, 91 (1981).
- ³⁹ L. E. Ballentine, *Quantum Mechanics: A Modern Development*, ch. 19 (1998).
- ⁴⁰ The energies of the emitted photons may in practice also be influenced by excitonic correlation effects that are beyond the scope of the present model. See, for example, Ref. 41.
- ⁴¹ B. L. Johnson and G. Kirczenow, *Phys. Rev. A* **54**, 241 (1996).
- ⁴² The implementation used was that of G.A. Landrum and W.V. Glassy, YAeHMOP project, <http://yaehmop.sourceforge.net>
- ⁴³ E. Kobayashi, Y. Terada, T. Ohashi and J. Furukawa, *Polymer Journal* **23**, 267 (1991).

FIGURES

FIG. 1. A schematic diagram of the model molecular wire. The source and drain contacts are semi-infinite. The two atoms in the center represent the molecule.

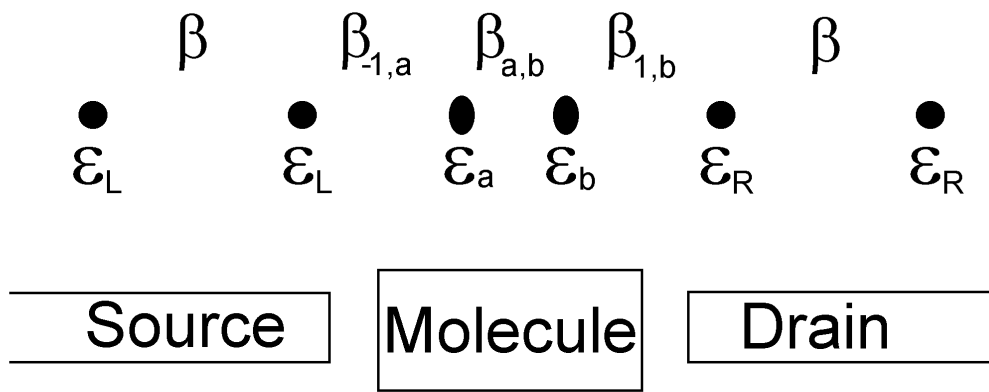
FIG. 2. Symmetrically coupled molecular wires for which at zero bias the HOMO-LUMO gap is centred at the Fermi level of the contacts and $\epsilon_{contacts} = \epsilon_a = \epsilon_b$. a) Source and drain electrochemical potentials μ_S and μ_D and energies of the bonding (O) and antibonding (O^*) orbitals as a function of bias voltage, for $\beta_{-1,a} = \beta_{1,b} = -1.0$ eV. b) Probability for the transmission of an electron through the molecular wire as a function of electron energy, for $V_{bias} = 0$ and $\beta_{-1,a} = \beta_{1,b} = -1.0$ eV. c) Occupations of the molecular bonding and antibonding orbitals, for $\beta_{-1,a} = \beta_{1,b} = -1.0$ eV, d) for $\beta_{-1,a} = \beta_{1,b} = -0.2$ eV. e) Total integrated photon emission, as a function of bias voltage, for (i) $\beta_{-1,a} = \beta_{1,b} = -0.2$ eV and (ii) $\beta_{-1,a} = \beta_{1,b} = -1.0$ eV. f) Emission spectra for various different bias voltages ($\beta_{-1,a} = \beta_{1,b} = -1.0$ eV).

FIG. 3. The case of E_F close to either the HOMO or LUMO at zero bias. $\beta_{-1,a} = \beta_{1,b} = -1.0$ eV for the entire figure. a) E_F is close to HOMO at zero bias. Energies of the bonding (O) and antibonding (O^*) orbitals as a function of bias voltage. b) Energies of O and O^* , for the case of E_F close to LUMO at zero bias. c) Occupations of O and O^* , for the situation in (a). d) Occupations of O and O^* , for the situation in (b). e) Total photon emission rate for the situation in (a) (emission rate for situation in (b) is very similar). f) Emission spectrum for the situation in (a) for $V_{bias} = 6$ V (Similar spectrum for situation in (b)).

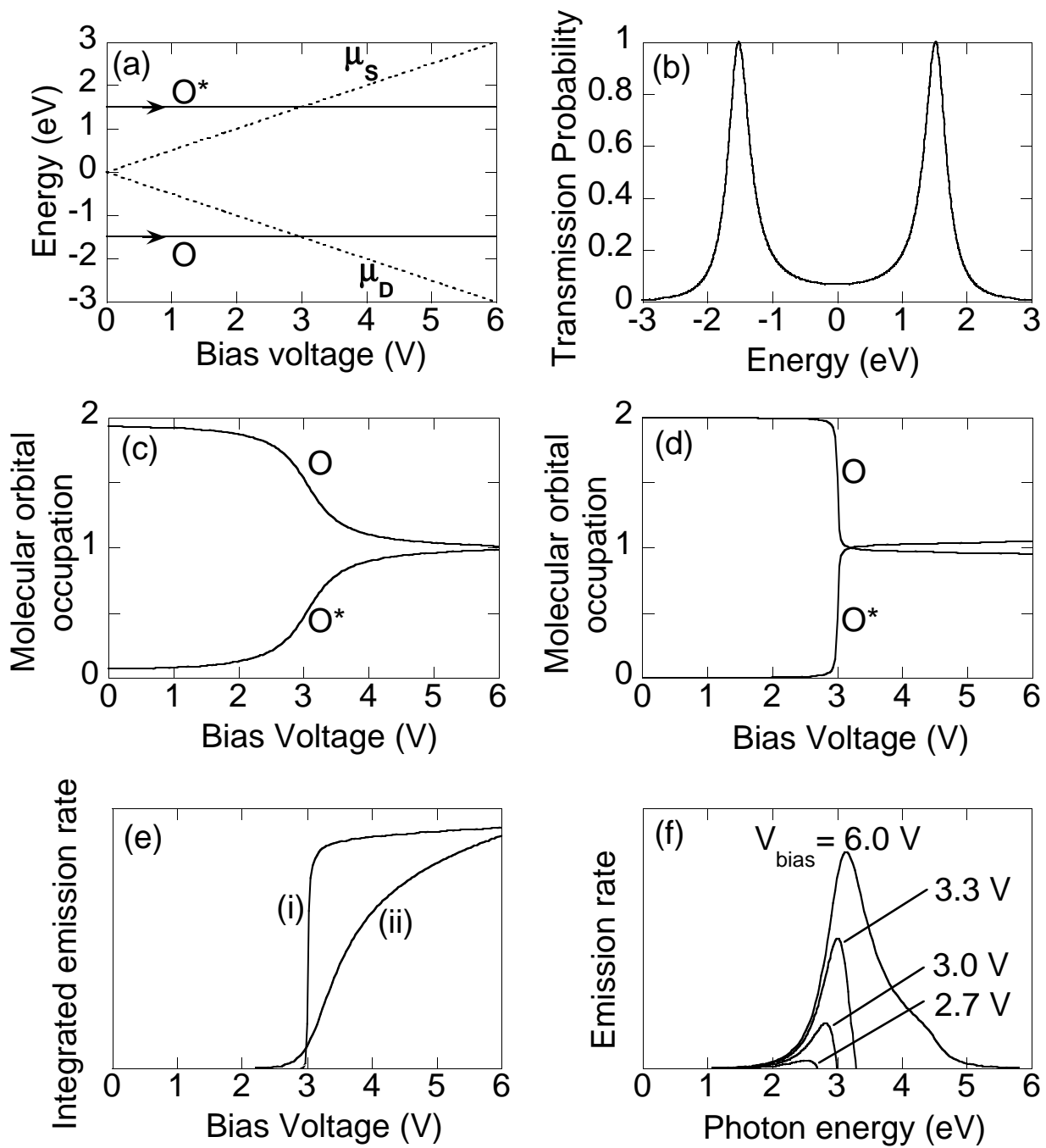
FIG. 4. The energies of O and O^* as a function of bias voltage, for the case of a HOMO LUMO gap that is centred at the zero bias Fermi level of the contacts, with highly asymmetric contact couplings ($\beta_{-1,a} = -0.1$ eV, $\beta_{1,b} = -1.0$ eV).

FIG. 5. The case of a HOMO-LUMO gap that is centred at the Fermi level of the contacts zero bias, for various asymmetric contact couplings. a) $\beta_{-1,a} = -0.6$ eV, $\beta_{1,b} = -1.0$ eV. Energies of the bonding (O) and antibonding (O^*) orbitals as a function of bias voltage. b) Occupations of O and O^* , corresponding to the situation in (a). c) Total photon emission rates, for various values of $\beta_{-1,a}$. $\beta_{1,b} = -1.0$ eV in all cases. d) Current for various values of $\beta_{-1,a}$. $\beta_{1,b} = -1.0$ eV in all cases. e) Photon emission (solid line) and current (dotted line) as a function of source contact coupling $\beta_{-1,a}$, for $\beta_{1,b} = -1.0$ V, $V_{bias} = 6$ V. Vertical scales are arbitrary. f) Total photon emission vs. current, for $\beta_{1,b} = -1.0$ V, $V_{bias} = 6$ V.

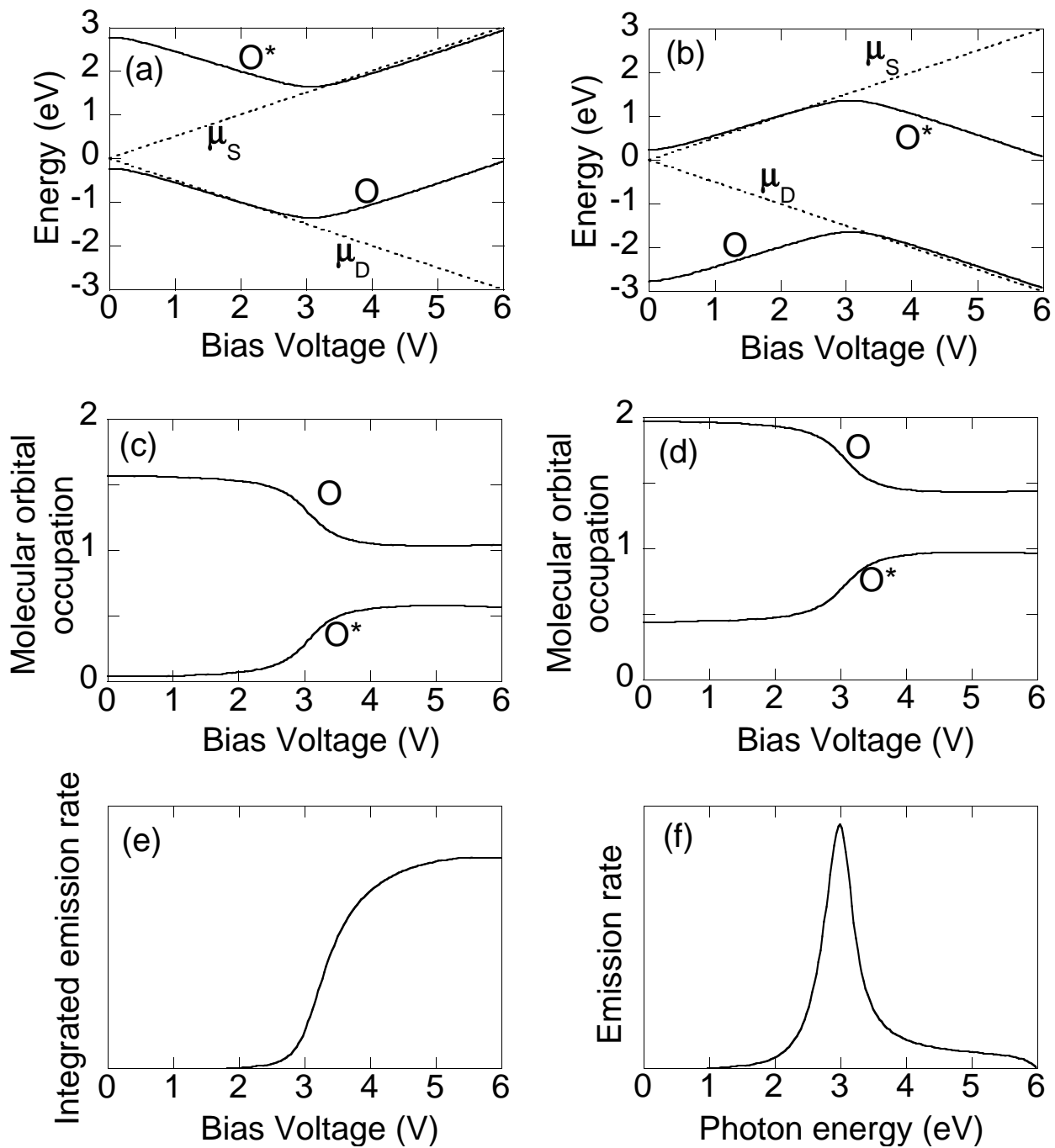
FIG. 6. a) The energies of O and O^* as a function of bias voltage, for the case of O located at E_F at zero bias, with highly asymmetric contact couplings ($\beta_{-1,a} = -0.1$ eV, $\beta_{1,b} = -1.0$ eV.) b) Energies of O and O^* for reversed couplings ($\beta_{-1,a} = -1.0$ eV, $\beta_{1,b} = -0.1$ eV). c) Total photon emission, corresponding to the situation in (a). d) Emission spectrum, corresponding to situation in (a), for $V_{bias} = 6$ V. e) Energies of O and O^* , for the case of O^* located at E_F at zero bias, with $\beta_{-1,a} = -0.1$ eV, $\beta_{1,b} = -1.0$ eV. f) Energies of O and O^* , for reversed couplings.



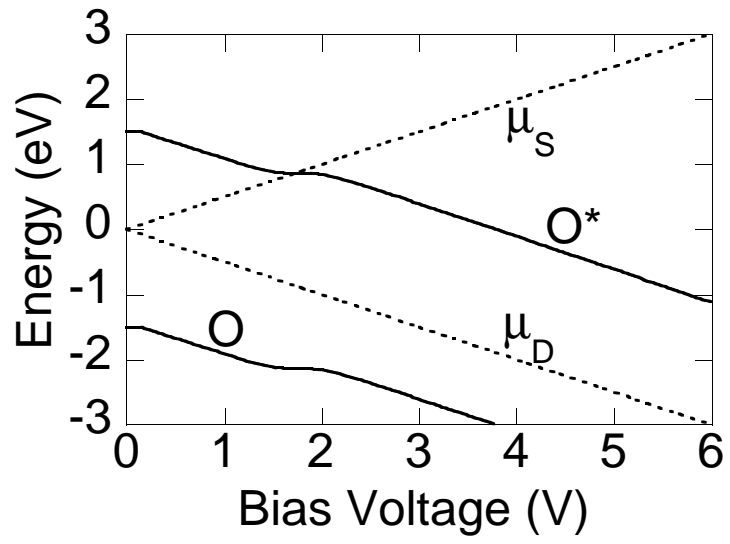
Buker and Kirczenow, Fig. 1



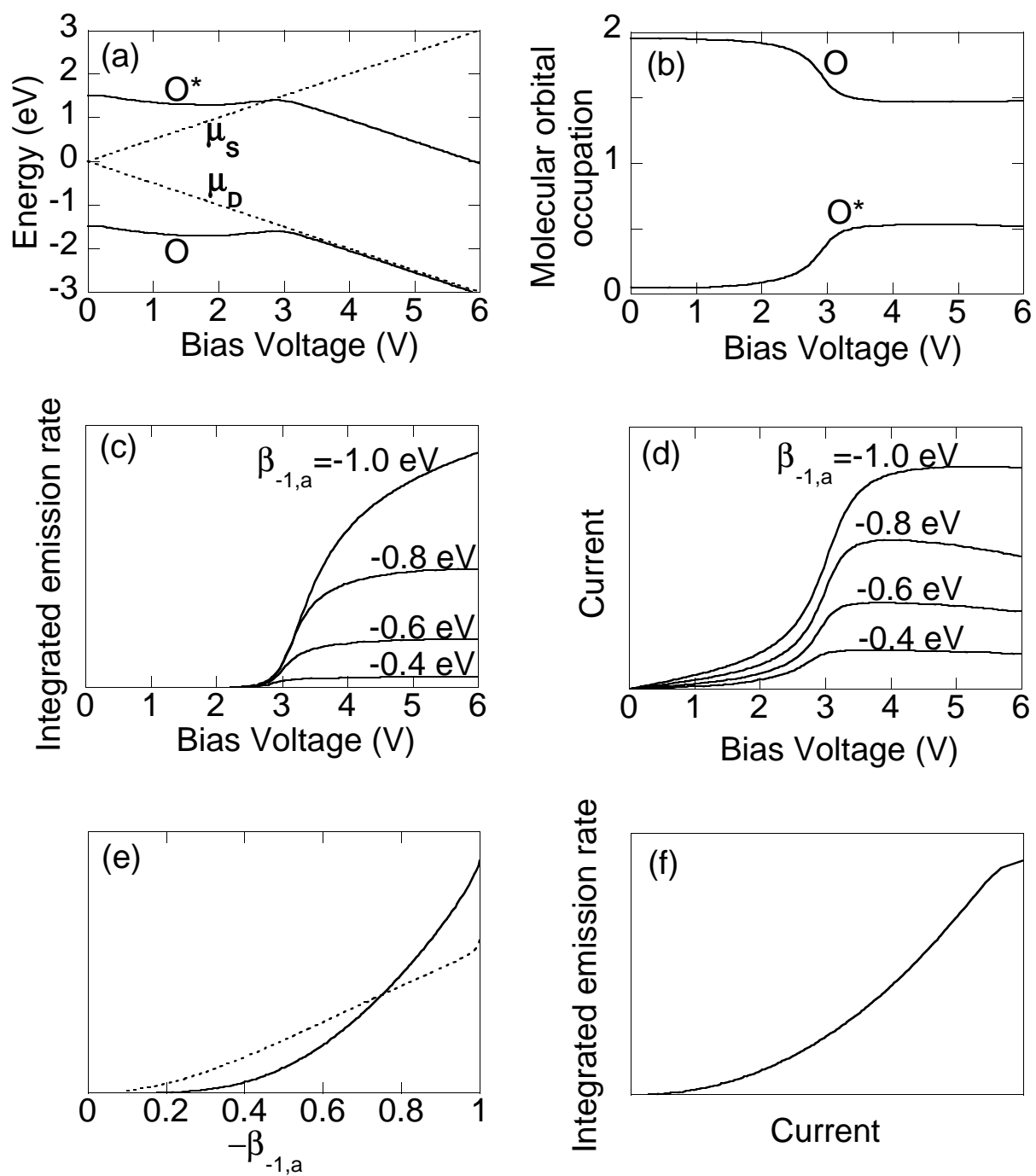
Buker and Kirczenow, Fig. 2



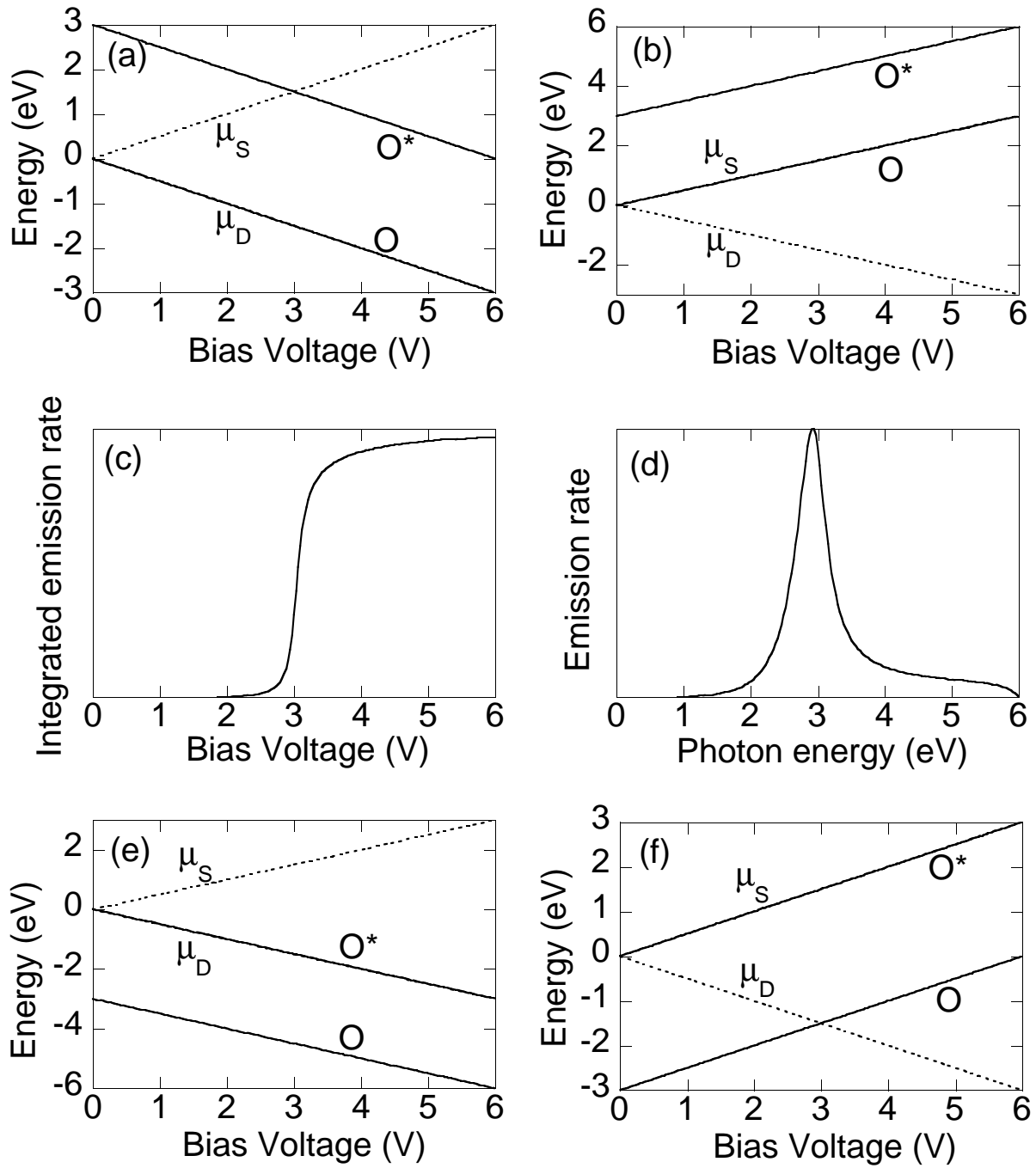
Buker and Kirczenow, Fig. 3



Buker and Kirczenow, Fig. 4



Buker and Kirczenow, Fig. 5



Buker and Kirczenow, Fig. 6